

Cellular-automaton model with velocity adaptation in the framework of Kerner's three-phase traffic theory

Kun Gao,^{1,*} Rui Jiang,^{2,†} Shou-Xin Hu,³ Bing-Hong Wang,^{1,‡} and Qing-Song Wu²

¹*Nonlinear Science Center and Department of Modern Physics, University of Science and Technology of China, Hefei, Anhui, 230026, People's Republic of China*

²*School of Engineering Science, University of Science and Technology of China, Hefei, Anhui, 230026, People's Republic of China*

³*Department of Science, Bengbu College, Bengbu, Anhui, 233050, People's Republic of China*

(Received 8 February 2007; revised manuscript received 5 June 2007; published 13 August 2007)

In this paper, we propose a cellular automata (CA) model for traffic flow in the framework of Kerner's three-phase traffic theory. We mainly consider the velocity-difference effect on the randomization of vehicles. The presented model is equivalent to a combination of two CA models, i.e., the Kerner-Klenov-Wolf (KKW) CA model and the Nagel-Schreckenberg (NS) CA model with slow-to-start effect. With a given probability, vehicle dynamical rules are changed over time randomly between the rules of the NS model and the rules of the KKW model. Due to the rules of the KKW model, the speed adaptation effect of three-phase traffic theory is automatically taken into account and our model can show synchronized flow. Due to the rules of the NS model, our model can show wide moving jams. The effect of "switching" from the rules of the KKW model to the rules of the NS model provides equivalent effects to the "acceleration noise" in the KKW model. Numerical simulations are performed for both periodic and open boundaries conditions. The results are consistent with the well-known results of the three-phase traffic theory published before.

DOI: [10.1103/PhysRevE.76.026105](https://doi.org/10.1103/PhysRevE.76.026105)

PACS number(s): 89.40.-a, 45.70.Vn, 05.40.-a, 02.60.Cb

I. INTRODUCTION

Traffic flow phenomena have attracted the interest of physicists since the early 1990s. Many models and analysis are carried out from the viewpoint of statistical physics by various groups recent years, in order to explain the empirical findings [1–12]. Among them, cellular automata (CA) models, as an important category, have become a well-established method to model, analyze, understand, and even forecast the behaviors of real road traffic since Nagel and Schreckenberg proposed a "minimal" CA model in 1992 which has become the basic model of this field and is called the Nagel-Schreckenberg (NS) model [13].

So far, most of these traffic models are due to the so-called "fundamental diagram approach," in which the steady state solutions belong to a curve in the flow-density plane [14–18]. Correspondingly, this curve going through the origin with at least one maximum is called "the fundamental diagram" for traffic flow.

The fundamental diagram approach is successful in explaining several aspects of real traffic, such as the forming of queue, the dissolution of jams, etc. The congested patterns from the fundamental diagram approach are due to the instability of steady states of the fundamental diagram within some range of vehicle densities. When perturbed, a transition from metastable free flow to jam ($F \rightarrow J$) occurs and the traffic decays into a single or a sequence of wide moving jams.

Nevertheless, a more detailed analysis of empirical data has been given by Kerner recently [8–12]. Based on these empirical data, it was found out that in congested traffic two

different traffic phases should be distinguished: "synchronized flow" and "wide moving jams." Therefore, there are three traffic phases: (1) free flow, (2) synchronized flow, (3) wide moving jams. Wide moving jams do not emerge spontaneously in free flow. Instead, there is a sequence of two first order phase transitions: first the transition from free flow to synchronized flow occurs ($F \rightarrow S$), and later and usually at a different location moving jams emerge in the synchronized flow ($S \rightarrow J$).

It is also pointed out by Kerner that the dynamical behavior near an on-ramp differs significantly in the fundamental diagram approach and in empirical observations. For example, in the diagram of congested states based on the fundamental diagram approach, at the highest values of on-ramp flow rate, the homogeneous congested traffic (HCT) occurs and no jam appears [15–18]. This is in contradiction with empirical observations where wide moving jams always emerge spontaneously in general pattern (GP) [4]. Moreover, at the low values of on-ramp flow rate, jams always emerge as a single moving local cluster (MLC) or triggered stop-and-go traffic (TSG) in the fundamental diagram approach [15–18]. However, synchronized patterns (SP) with high speed and flow rate that is as great as in free flow appear in empirical observations in which no wide moving jams occur [4].

Based on empirical observations, Kerner developed a three-phase traffic theory [19–24]. The fundamental hypothesis of this theory is that the steady states of synchronized flow cover a two-dimensional (2D) region in the flow-density plane [25,26]. That is to say, a fundamental diagram of traffic flow in this theory does not exist. In a traffic model based on this theory, moving jams do not spontaneously occur in free flow. Instead, the first-order phase transition to synchronized flow beginning at some density in free flow is realized. The moving jams emerge only in synchronized

*kgao@mail.ustc.edu.cn

†rjiang@ustc.edu.cn

‡bhwang@ustc.edu.cn

flow. As a result, the diagrams of traffic patterns both for a homogeneous road without bottlenecks and at on-ramps are qualitatively different from those found in the fundamental diagram approach. Kerner believes that a model within the framework of three-phase traffic theory should be able to (at least qualitatively) reproduce the empirical observed spatiotemporal patterns.

In 2002, Kerner and Klenov developed a microscopic model of the three-phase traffic theory, which can reproduce empirical spatiotemporal patterns [27]. Later, microscopic models based on three phase traffic theory have been developed, such as the Kerner-Klenov-Wolf (KKW) CA model [19,28], the CA model introduced by Lee *et al.* [29], which considers the mechanical restriction versus human overreaction, the model proposed by Davis [30], the model of Jiang and Wu [31,32], and the deterministic models proposed by Kerner and Klenov [33]. As in empirical observations, these models exhibit the sequence of $F \rightarrow S \rightarrow J$ transitions leading to wide moving jams emergence beginning from free flow. In addition, the models show all types of congested patterns found in empirical observations.

In this paper, we are going to propose another CA model on the basis of the existing models in the framework of three-phase traffic theory. We mainly consider the velocity-difference effect on the randomization of vehicles in this model. It will be shown later that the presented model is equivalent to a combination of two CA models, i.e., the KKW model [19,28] and the NS model with slow-to-start effect [34]. This model can show both synchronized flow and wide moving jams, which will be exhibited in the latter part of this paper.

The rest of this paper is organized as follows. In Sec. II, we describe our model. In Sec. III, simulations on roads under both periodic and open boundary conditions are presented. In Sec. IV, we conclude.

II. THE MODEL

In this section we present our model. The main mechanisms associated with three-phase traffic theory in this model are embodied in the randomization process of vehicles. The parallel update rules are as follows.

(1) Determining the randomization probability $p_n(t+1)$ and the deceleration extent Δv .

$$p_n(t+1) = \begin{cases} p_0 & \text{when } t_{st,n} \geq t_c, \\ p_d & \text{when } t_{st,n} < t_c, \end{cases} \quad (1)$$

$$\Delta v = \begin{cases} a & \text{when } t_{st,n} \geq t_c \\ \left. \begin{array}{l} b_- \text{ if } [v_n(t) < v_{n-1}(t)] \\ b_0 \text{ if } [v_n(t) = v_{n-1}(t)] \\ b_+ \text{ if } [v_n(t) > v_{n-1}(t)] \end{array} \right\} & \text{when } t_{st,n} < t_c. \end{cases} \quad (2)$$

(2) Accelerating:

$$v_n(t+1) = \min[v_n(t) + a, v_{\max}].$$

(3) Braking:

$$v_n(t+1) = \min[v_n(t+1), d_n].$$

(4) Randomization with probability $p_n(t+1)$:

$$v_n(t+1) = \max[v_n(t+1) - \Delta v, 0].$$

(5) The determination of $t_{st,n}$:

$$t_{st,n} = \begin{cases} t_{st,n} + 1 & \text{if } [v_n(t+1) = 0] \\ 0 & \text{if } [v_n(t+1) > 0]. \end{cases} \quad (3)$$

(6) Vehicle motion:

$$x_n(t+1) = x_n(t) + v_n(t+1).$$

Here $x_n(t)$ and $v_n(t)$ are the position and velocity of vehicle n at time t (here vehicle $n-1$ precedes vehicle n), d_n is the gap of vehicle n , i.e., the distance from the head of vehicle n to the tail of vehicle $n-1$, $t_{st,n}$ denotes the time that vehicle n stops, and t_c is a slow-to-start parameter. The following rank of the acceleration and deceleration parameters are required:

$$b_+ \geq a \geq b_-. \quad (4)$$

In the rules above, Eqs. (1) and (3) represent the slow-to-start effect. Following the work of Jiang and Wu, it is fulfilled by considering the stop times of vehicles. In our viewpoint, the driver's attention will be kept concentrated when encountering short-time halt in traffic, but distracted after a long time waiting. (For example, someone may read a newspaper or even go out of the car. This is simulated by large randomization.) So the slow-to-start would happen only with a long stop time. The threshold parameter t_c is set for this. We will discuss on the effect of t_c later.

On the other hand, Eqs. (2) and (4) describe the speed adaptation effect. When the velocity is larger than the velocity of the leading vehicle, the driver will tend to overreact when decelerating. The deceleration extent will be relatively large, corresponding to the largest parameter b_+ . In order to simulate the synchronized flow, Eq. (4) is sufficient and necessary. As a result, when randomization occurs, the vehicle will adjust its velocity close to the velocity of the leading vehicle. This is consistent with the basic rules of the KKW model [19,28].

Actually, the presented model is equivalent to a combination of two existing CA models, i.e., the KKW model and the NS model with slow-to-start effect. To show this, we consider our model in the intermediate range of vehicle speed, which are the most interesting for simulations of synchronized flow. When $v_n(t) + a \leq v_{\max}$, $v_n(t) + a \leq d_n$, and $t_{st,n} < t_c$, namely, there are no restrictions related to the maximum speed v_{\max} and the safe speed d_n , respectively, and also no slow-to-start rule, the updating rule of our model is

$$v_n(t+1) = v_n(t) + \begin{cases} a - b_- \geq 0 & \text{if } [v_n(t) < v_{n-1}(t)], \\ a - b_0 & \text{if } [v_n(t) = v_{n-1}(t)], \\ a - b_+ \leq 0 & \text{if } [v_n(t) > v_{n-1}(t)] \end{cases} \quad (5)$$

with probability p_d or

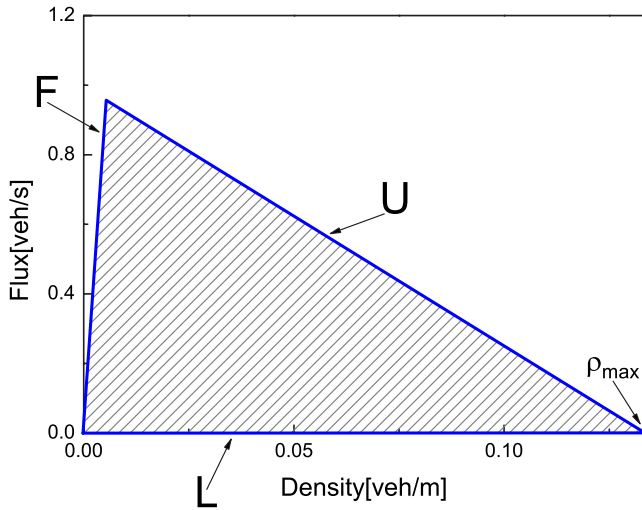


FIG. 1. (Color online) The two-dimensional region of the equilibrium states of synchronized flow in a noiseless limit, in which $p_d \rightarrow 1$. Assuming the length of a single vehicle is 7.5 m and the maximum velocity is 37.5 m/s.

$$v_n(t+1) = v_n(t) + a \quad (6)$$

with probability $1 - p_d$.

Equation (5) above is exactly the basic rule of the KKW model when $a = b_0$ and $|a - b_-| = |a - b_+|$. In this case, the speed adaptation effect of three-phase traffic theory is automatically taken into account. Synchronized flow could be simulated due to these rules. It should be noted that the condition $a = b_0$ is not necessary for simulating synchronized flow in our model (although we happen to adopt parameters satisfying this condition when enumerating simulation results in the next part of this paper).

On the other hand, Eq. (6), also including the $t_{st,n} \geq t_c$ cases, corresponds to the NS model. Due to these rules, wide moving jams can be simulated.

Thus in the presented model, the vehicle motion rules are switched between the rules of the NS model and the rules of the KKW model with probabilities. At a certain time, the rules of the KKW model are adopted with probability p_d , and the rules of the NS model are adopted with probability $1 - p_d$. The “switching” of the rules from the KKW model to the NS model can be regarded as an additional acceleration, which provides equivalent effects as the “acceleration noise” in the initial KKW model. On the other hand, the “deceleration noise” in the KKW model can also be implemented by setting the parameters as $|a - b_+| > |a - b_-|$. However, through simulations we found it not absolutely necessary for reproducing synchronized flow in our model.

The fundamental hypothesis of Kerner’s three-phase traffic theory is that the equilibrium states (homogeneous and stationary states, time-independent solutions in which all vehicles move with the same constant speed) of synchronized flow cover a two-dimensional region in the flow-density plane [25,26]. In what follows, we will show the steady states of this model cover a two-dimensional region in the flow-density plane in a noiseless limit. Because the mechanisms associated with the synchronized flow in this model

are all embodied in the randomization process, the noiseless limit is taken as $p_d \rightarrow 1$ rather than $p_d \rightarrow 0$. In this case, the updating rules of the KKW model are adopted. As shown in Refs. [19,27], the two-dimensional region of the equilibrium states is restricted by three boundaries in the flow-density plane: the upper (line U), the lower (line L), and the left (line F) boundaries. Compared to the basic rule of the KKW model, the only difference in the rules of our model is that there does not exist such a parameter as the synchronization distance $D(v)$, which describes the maximal distance at which the vehicle takes into account the speed of the leading vehicle when accelerating [19,27]. In other words, our model can be regarded as a limit of the KKW model when $D(v) \rightarrow \infty$. As a result, the lower boundary L of the two-dimensional region approaches the x axis.

As in the KKW model, the upper boundary U is determined by the safe speed of vehicles, which is determined by the headway distance (in equilibrium states, we assume all the vehicles have a uniform speed and headway distance). Thus the line U is determined by

$$v = d = \frac{1}{\rho} - l,$$

where ρ is the density of vehicles and l is the length of a single vehicle. Therefore, in the flow-density plane, the flux

$$J_U(\rho) = v\rho = 1 - \rho l$$

and the left boundary F corresponds to the free flow speed $v_{\text{free}} = v_{\text{max}}$, thus

$$J_F(\rho) = \rho v_{\text{max}}.$$

The two-dimensional region of equilibrium states is restricted by these three boundaries, as shown in Fig. 1.

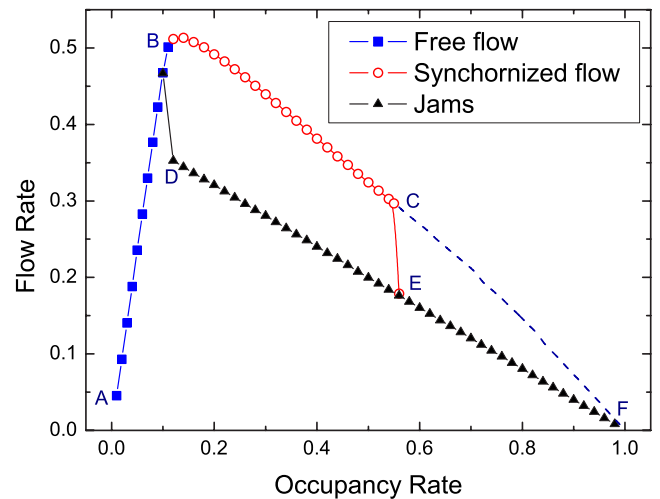


FIG. 2. (Color online) The fundamental diagram of our model, obtained on a circular road by starting from two different initial states: completely jammed states (low branch) and homogeneous states (upper branch). The dashed line CF belongs to the simulation results for extremely large t_c . When t_c increases, point C moves rightward along CF , until the synchronized branch covers the whole segment BCF when t_c is large enough (see text).

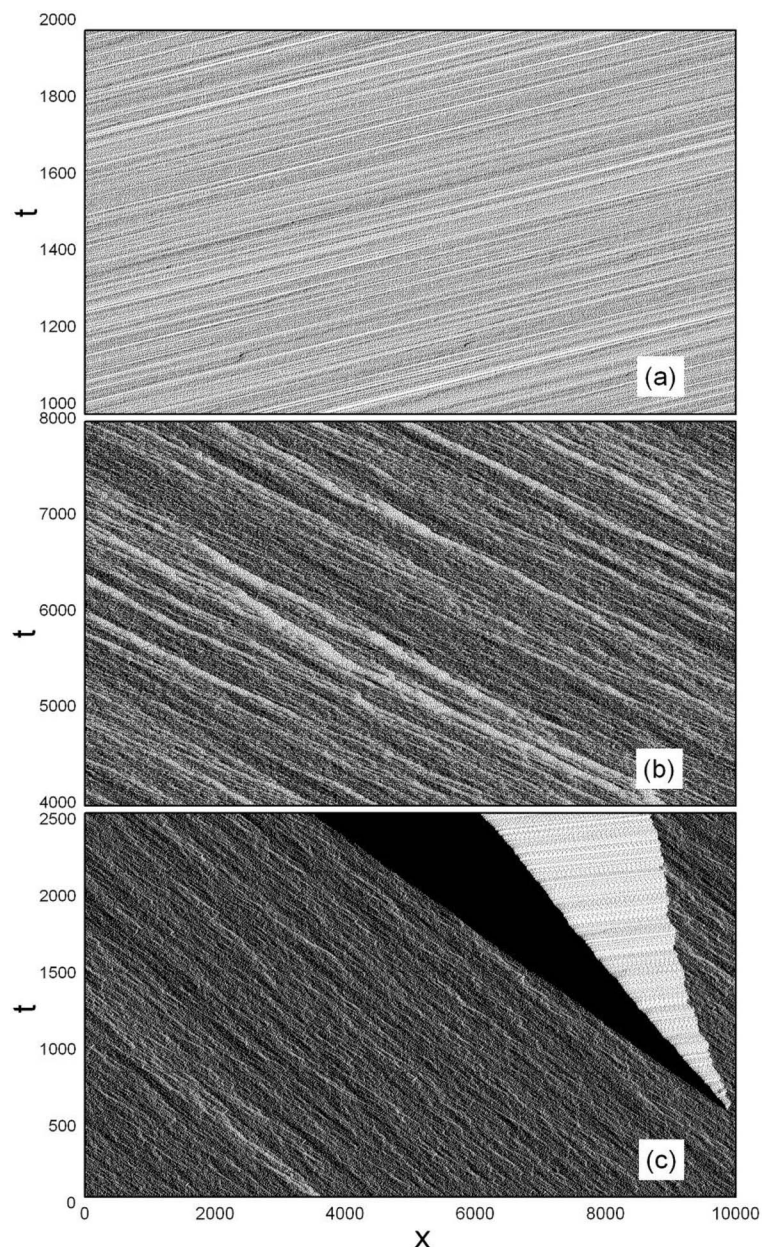


FIG. 3. The spatial-temporal diagrams of our model on a circular road, all starting from homogeneous initial states. (a) The free flow phase when $\rho=0.08$. (b) The synchronized flow phase when $\rho=0.4$. (c) The synchronized flow spontaneously evolves into the jam when $\rho=0.55$.

In the following section, simulations are carried out on a road of 10 000 cells. Both periodic and open boundary conditions are used. Each cell corresponds to 1.5 m and a vehicle has a length of five cells. One time step corresponds to 1 s. The parameters are set as $t_c=7$, $v_{\max}=25$, $p_d=0.3$, $p_0=0.6$, $a=2$, $b_-=1$, $b_0=2$, and $b_+=5$.

III. SIMULATION RESULTS

In this section, simulations are carried out. We first show the simulation results on a circular road with periodic boundary conditions. Figure 2 shows the fundamental diagram of the new model. Branch (A-B-C) is obtained from homogeneous initial states; and branch (D-E-F) is obtained from megajams. Each data point is an average over 20 individual runs with 2000 time steps for each run after 10 000 time steps' evolution. Hysteresis effect occurs in the diagram.

Three different phases of traffic, i.e., free flow (branch AB), synchronized flow (branch BC), and jams (branch DEF) are distinguished, and the first order transition (C to E) from synchronized flow to jams is exhibited (see the double Z-shaped characteristics of traffic flow in Chaps. 6 and 17 in Ref. [4]).

The corresponding spatial-temporal patterns are shown in Fig. 3. Figures 3(a) and 3(b) show the spatial-temporal characters of free flow and synchronized flow (SP, see Chap. 7 in Ref. [4]), respectively, and Fig. 3(c) exhibits the spontaneous transition from synchronized flow to jams (namely, the so-called GP, see Chap. 18 in Ref. [4]).

We investigate the effect of t_c on the fundamental diagram. The value of t_c will influence the length of the synchronized branch in the flow-density plane (i.e., the location of point C in Fig. 2), and the probability for jams to spontaneously occur in synchronized flow. With the increase of t_c , point C moves rightward along the dashed line CF in Fig. 2,

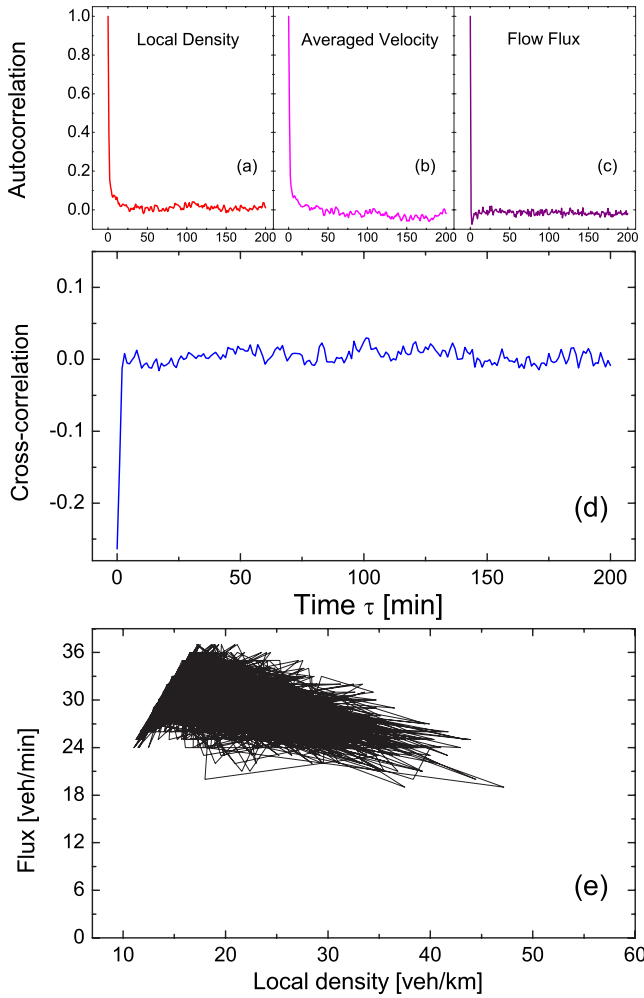


FIG. 4. (Color online) (a)–(c) Autocorrelation functions of one-minute aggregates of local density, average velocity, and flow flux of synchronized flow, respectively. (d) Cross-correlation function between density and flux of the synchronized flow. (e) One-minute averaged flux-density diagram corresponding to the synchronized flow in (a)–(d). The global density is $\rho=0.14$.

and the rest part of the upper branch (*ABC*) remains unaltered approximately. When t_c is large enough, *C* approaches *F*. At the same time, it becomes more and more difficult for wide moving jams to spontaneously emerge in a homogeneous traffic. On the other hand, with the decrease of t_c , *C* moves leftward, and finally approaches *B*. The model reduces to a model similar to the velocity-dependent randomization (VDR) model [34] when t_c is small enough.

Next we study the microscopic statistical characteristics of the simulated synchronized flow. Time series obtained through a fixed virtual loop detector are analyzed. First we consider the autocorrelation function

$$a_x(\tau) = \frac{\langle x(t)x(t+\tau) \rangle - \langle x(t) \rangle^2}{\langle x(t)^2 \rangle - \langle x(t) \rangle^2}$$

of the aggregated quantities $x(t)$ [35]. The brackets $\langle \dots \rangle$ indicate the average over the whole series of x . In Figs. 4(a)–4(c), the autocorrelations of one-minute aggregates of

the density, average velocity, and flow flux of a synchronized state are shown. We can see the autocorrelations are all close to zero, which means no long-range correlations exist. Moreover, Fig. 4(d) shows that the cross-correlation function

$$c_{xy}(\tau) = \frac{\langle x(t)y(t+\tau) \rangle - \langle x(t) \rangle \langle y(t) \rangle}{\sqrt{\langle x(t)^2 \rangle - \langle x(t) \rangle^2} \sqrt{\langle y(t)^2 \rangle - \langle y(t) \rangle^2}}$$

between density and flux vanishes in large time scale [35]. Both functions exhibit characteristics of synchronized flow (see Ref. [35]; neither the free flow nor the jams have zero-valued correlation functions characteristically). Figure 4(e) shows the one-minute averaged flow-density diagram covering a two-dimensional region in the flow-density plane, which is consistent with the fundamental hypothesis of three-phase traffic theory [25,26].

Next we show the simulated features induced by an on-ramp under open boundary conditions. The open boundary conditions are applied as follows. Assuming the left-most cell on the road corresponds to $x=1$ and the position of the left-most vehicle is x_{last} , a new vehicle with velocity v_{max} will be injected to the position $\min\{x_{\text{last}} - v_{\text{max}}, v_{\text{max}}\}$ with probability q_{in} , if $x_{\text{last}} > v_{\text{max}}$. The stop time t_{st} of the newly injected vehicle is set to zero. At the right boundary, the leading vehicle moves without any hindrance. When the position of the leading vehicle $x_{\text{lead}} > L$, in which L corresponds to the position of the exit, it will be removed and the second vehicle becomes the leader.

At the on-ramp, we adopt a simple setup. At each time step, we scan the region of the on-ramp $[x_{\text{on}} - L_{\text{ramp}}, x_{\text{on}}]$ and find out the longest gap in this region. If this gap is long enough for a vehicle, then a new vehicle will be injected into the cells in the middle of the gap with probability q_{on} . The velocity of the newly injected vehicle is set to equal the velocity of its preceding vehicle, and the stop time is set to zero. In this paper, we set $x_{\text{on}}=0.8L$ and $L_{\text{ramp}}=30$.

With such an isolated on-ramp, this model can simulate the congested patterns predicted by three-phase traffic theory. Figure 5 is the diagram of traffic patterns induced by the on-ramp. The $q_{\text{on}}-q_{\text{in}}$ plane is divided into six regions, corresponding to six different traffic patterns, shown, respectively, in the spatial-temporal diagrams in Fig. 6.

In region I in Fig. 5, free flow covers the whole road. In region II, a congested pattern occurs where synchronized flow appears upstream of the on-ramp and wide moving jams spontaneously emerge in the synchronized flow. This pattern is named the “general pattern” (GP) as it contains both phases (synchronized flow and wide moving jams) of the congested traffic (see Chap. 18 in Ref. [4]). In the GP, synchronized flows are bounded by a sequence of wide moving jams. The downstream fronts of the jams move upstream with a constant speed. The region of GP is continuously widening upstream. Spatial-temporal features of GP are shown in Fig. 6(a).

When q_{on} is not so large, wide moving jams do not emerge in synchronized flow. There is only synchronized flow upstream the on-ramp. These patterns are called the “synchronized flow patterns” (SP) (see Chap. 7 in Ref. [4]),

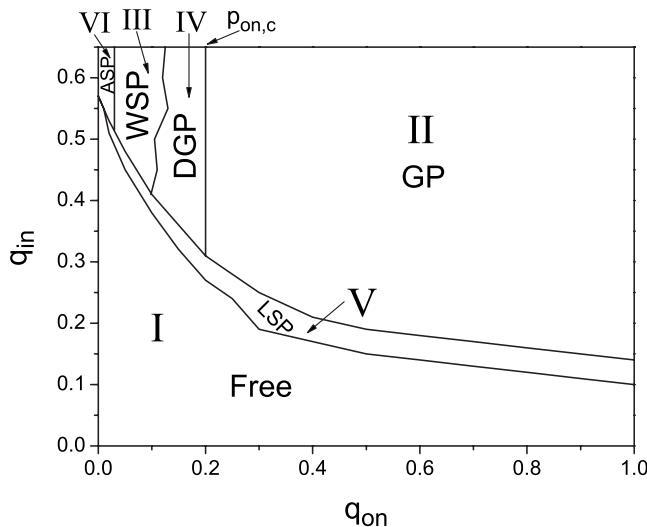


FIG. 5. Diagram of traffic patterns induced by an isolated on-ramp. Free: Free flow; GP: General pattern; WSP: Widening synchronized flow pattern; DGP: Dissolving general pattern; LSP: Localized synchronized flow pattern; ASP: Synchronized flow pattern with alternations of free and synchronized flow.

consisting of three patterns corresponding to regions III, IV, V in Fig. 5.

As Fig. 6(b) shows, in region III, the downstream front of the synchronized flow is fixed at the on-ramp and the upstream front is continuously widening upstream. This pattern is named the “widening synchronized flow pattern” (WSP). When the values of q_{on} are within the intergrade between WSP and GP, as in region IV in Fig. 5, another pattern called the “dissolving general pattern” (DGP) occurs. In this pattern, the transition from synchronized flow to jams occurs inside the WSP. But it could not induce wide moving jams sequences, but only a jamming area dissolving over time, as Fig. 6(c) shows. As the outflow rate of the jam is smaller than the capacity of the on-ramp system, free flow occurs between the on-ramp and the downstream front of the jam. The boundary between regions II and IV is a vertical line which intersects x axis at the point $p_{on,c}$. Upon this boundary, the capacity of the on-ramp system equals to the outflow rate of the jams.

A fourth congested pattern occurs in region V. As shown in Fig. 6(d), the downstream front of the synchronized flow is also fixed at the on-ramp and no jams emerge in the synchronized flow. However, in contrast to the WSP, the upstream front of this synchronized flow is not continuously widening over time, but limited somewhere upstream of the on-ramp. The whole synchronized region is localized near the on-ramp. So this pattern is called the “localized synchronized flow pattern” (LSP). Figure 6(d) also shows that the width of LSP, or say, the position of the upstream front of LSP, depends on time and exhibits complex fluctuations with large amplitude.

When q_{in} is large and q_{on} is small, a fifth congested pattern occurs in region VI. Free flow emerges inside the synchronized region. A spatially mixture of free flow and synchronized flow covers the road [Fig. 6(e)]. At a fixed position on the road, one will observe alternative regions of free flow

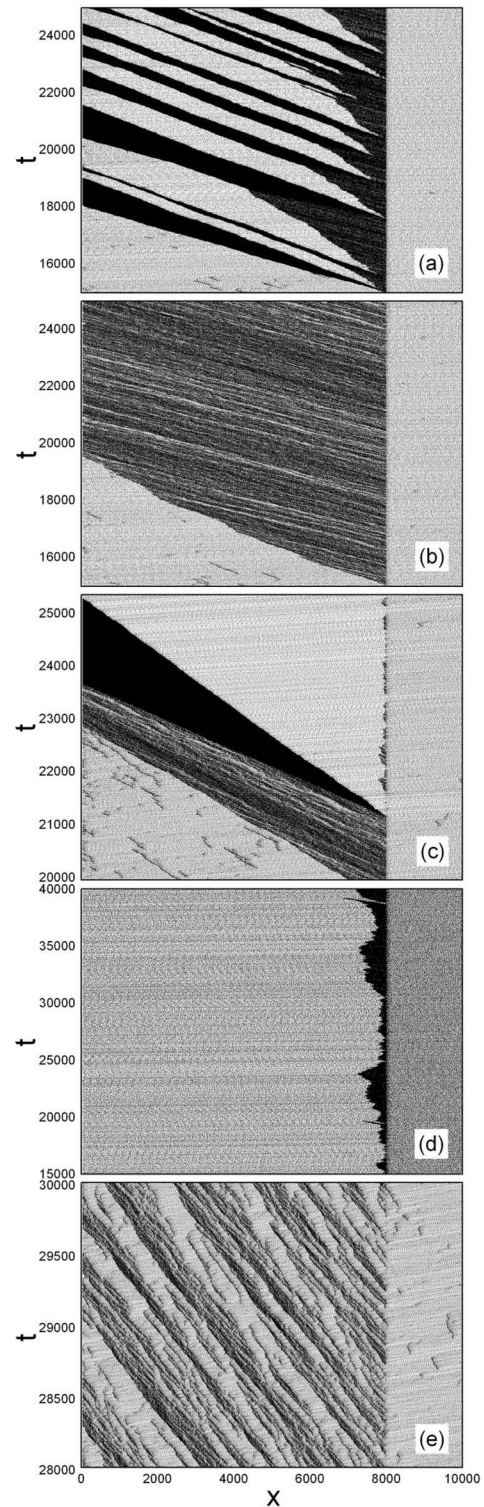


FIG. 6. The spatial-temporal diagram of the congested patterns. (a) GP, (b) WSP, (c) DGP, (d) LSP, (e) ASP. The parameter is (a) $q_{in}=0.50$, $q_{on}=0.30$, (b) $q_{in}=0.50$, $q_{on}=0.12$, (c) $q_{in}=0.60$, $q_{on}=0.10$, (d) $q_{in}=0.30$, $q_{on}=0.20$, (e) $q_{in}=0.60$, $q_{on}=0.04$.

and synchronized flow. Therefore, it is called “SP with alternations of free and synchronized flow” (ASP).

It should be noted that the boundaries in Fig. 5 are not absolutely rigorous. In fact, near the boundaries, both patterns could exist. Especially near the boundary between re-

regions III and IV, both WSP and DGP could occur under the same set of parameters. Different random seeds could exhibit different patterns (i.e., WSP and/or DGP occur with certain probability at given parameters near the boundary between regions III and IV).

Compared with the well-known results of the three-phase traffic theory published before, the pattern diagram in Fig. 5 and the spatial-temporal patterns in Fig. 6 are all qualitatively consistent with the theory [4]. So we believe this model is efficient and reliable in the framework of three-phase traffic theory.

IV. CONCLUSIONS

In this paper, we have proposed a cellular automaton model for traffic flow within the framework of three-phase traffic theory. The velocity-difference effect on the randomization of vehicles is the most essential part of this model. This model is found to be equivalent to a combination of two CA models, i.e., the KKW model and the Nagel-Schreckenberg model with slow-to-start effect. Due to the rules of the KKW model, our model can show synchronized flow. Due to the rules of the Nagel-Schreckenberg model, our model can show

wide moving jams. With a certain probability, this model switches between the rules of the KKW model and the Nagel-Schreckenberg model, which provides equivalent effects as the “acceleration noise” in the initial KKW CA model.

This model can reproduce synchronized flow, and multiple congested patterns induced by an isolated on-ramp. The results are well consistent with the well-known results of the three-phase traffic theory published before.

However, some other important features of traffic have not been exhibited by this simple model. For example, the first order transition from free flow to synchronized flow is not reproduced. These features need to be investigated in future work.

ACKNOWLEDGMENTS

This work was funded by the National Basic Research Program of China (973 Program No. 2006CB705500), the National Natural Science Foundation of China (Grant Nos. 10635040, 10532060, 10472116, 10404025), by the Special Research Funds for Theoretical Physics Frontier Problems (NSFC Grant No. 10547004 and A0524701), by the President Funding of Chinese Academy of Science, and by the Specialized Research Fund for the Doctoral Program of Higher Education of China.

-
- [1] *Traffic and Granular Flow 97*, edited by M. Schreckenberg and D. E. Wolf (Springer, Singapore, 1998); *Traffic and Granular Flow 99*, edited by D. Helbing, H. J. Herrmann, M. Schreckenberg, and D. E. Wolf (Springer, Berlin, 2000).
 - [2] D. Chowdhury, L. Santen, and A. Schadschneider, *Phys. Rep.* **329**, 199 (2000).
 - [3] D. Helbing, *Rev. Mod. Phys.* **73**, 1067 (2001).
 - [4] B. S. Kerner, *The Physics of Traffic* (Springer, Berlin, 2004).
 - [5] L. C. Edie, *Oper. Res.* **9**, 66 (1961).
 - [6] J. Treiterer and J. A. Myers, in *Proceedings of the 6th International Symposium on Transportation and Traffic Theory*, edited by D. Buckley (Reed, London, 1974), p. 13.
 - [7] M. Koshi, M. Iwasaki, and I. Ohkura, in *Proceedings of the 8th International Symposium on Transportation and Traffic Flow Theory* (University of Toronto Press, Toronto, 1983), p. 403.
 - [8] B. S. Kerner and H. Rehborn, *Phys. Rev. Lett.* **79**, 4030 (1997).
 - [9] B. S. Kerner and H. Rehborn, *Phys. Rev. E* **53**, R1297 (1996).
 - [10] B. S. Kerner and H. Rehborn, *Phys. Rev. E* **53**, R4275 (1996).
 - [11] B. S. Kerner, *Phys. Rev. Lett.* **81**, 3797 (1998).
 - [12] B. S. Kerner, *Phys. Rev. E* **65**, 046138 (2002).
 - [13] K. Nagel and M. Schreckenberg, *J. Phys. I* **2**, 2221 (1992).
 - [14] P. Berg and A. Woods, *Phys. Rev. E* **64**, 035602(R) (2001).
 - [15] D. Helbing, A. Hennecke, and M. Treiber, *Phys. Rev. Lett.* **82**, 4360 (1999).
 - [16] M. Treiber, A. Hennecke, and D. Helbing, *Phys. Rev. E* **62**, 1805 (2000).
 - [17] H. Y. Lee, H. W. Lee, and D. Kim, *Phys. Rev. Lett.* **81**, 1130 (1998).
 - [18] H. Y. Lee, H. W. Lee, and D. Kim, *Phys. Rev. E* **59**, 5101 (1999).
 - [19] B. S. Kerner, S. L. Klenov, and D. E. Wolf, *J. Phys. A* **35**, 9971 (2002).
 - [20] B. S. Kerner, H. Rehborn, M. Aleksic, and A. Haug, *Transp. Res., Part C: Emerg. Technol.* **12**, 369 (2004).
 - [21] B. S. Kerner, H. Rehborn, A. Haug, and I. Maiwald-Hiller, *Traffic Eng. Control* **46**, 380 (2005).
 - [22] B. S. Kerner, S. L. Klenov, A. Hiller, and H. Rehborn, *Phys. Rev. E* **73**, 046107 (2006).
 - [23] B. S. Kerner, S. L. Klenov, and A. Hiller, *J. Phys. A* **39**, 2001 (2006).
 - [24] H. Rehborn, http://www.dlr.de/fs/PortalData/16/Resources/dokumente/vk/vp_fs_ex_Vortrag_Rehborn_050407.pdf
 - [25] B. S. Kerner in *Proceedings of the 3rd Symposium on Highway Capacity and Level of Service*, edited by R. Rysgaard (Road Directorate, Ministry of Transport, Denmark, 1998), Vol. 2, pp. 621–642.
 - [26] B. S. Kerner, *Transp. Res. Rec.* **1678**, 160 (1999).
 - [27] B. S. Kerner and S. L. Klenov, *J. Phys. A* **35**, L31 (2002).
 - [28] B. S. Kerner, *Physica A* **333**, 379 (2004).
 - [29] H. K. Lee, R. Barlovic, M. Schreckenberg, and D. Kim, *Phys. Rev. Lett.* **92**, 238702 (2004).
 - [30] L. C. Davis, *Phys. Rev. E* **69**, 016108 (2004).
 - [31] R. Jiang and Q. S. Wu, *J. Phys. A* **36**, 381 (2003).
 - [32] R. Jiang and Q. S. Wu, *Eur. Phys. J. B* **46**, 581 (2005).
 - [33] B. S. Kerner and S. L. Klenov, *J. Phys. A* **39**, 1775 (2006).
 - [34] R. Barlović, L. Santen, A. Schadschneider, and M. Schreckenberg, *Eur. Phys. J. B* **5**, 793 (1998).
 - [35] L. Neubert, L. Santen, A. Schadschneider, and M. Schreckenberg, *Phys. Rev. E* **60**, 6480 (1999).